CARAS
© 2023, Centre for Advanced Research in Agricultural Sciences
Research Journal of Agricultural Sciences
Volume 14; Issue 03 (May-Jun 2023); pp 711–715

Open Access
ISSN: 0976-1675 (P)
ISSN: 2249-4538 (E)

Full Length Research Article

Barium Modified Titanium Dioxide Nanoparticles Prepared Via a Green Process using *Withania somnifera* Hairy Roots

Raja Palusamy[1], Thiagu Ganesan[2], Liyahathalikhan Umaralikhan[3] and Appakan Shajahan*[4]

[1-2,4] Plant Molecular Biology Laboratory, P. G. and Research Department of Botany, Jamal Mohamed College (Autonomous), Affiliated to Bharathidasan University, Tiruchirappalli - 620 020, Tamil Nadu, India
[3] PG and Research Department of Physics, Jamal Mohamed College (Autonomous), Affiliated to Bharathidasan University, Tiruchirappalli, Tamil Nadu, India

Abstract

In the current work, green processed of Ba-modified TiO_2 nanoparticles (GBT) was employed from aqueous *Withania somnifera* hairy roots (WSR). The GBT was characterized by different methods such as X-ray diffraction (XRD) studies, SEM and energy-dispersive X-ray analysis (EDX), dynamic light scattering (DLS), Fourier transform infrared (FTIR) spectroscopy, ultraviolet (UV) spectroscopy, and photoluminescence (PL) spectra. The crystallites exhibited a size of 65–75 nm measured via DLS, while SEM with EDX analysis of synthesized nanoparticles confirmed their spherical-shaped and bowl-like particles. Using FTIR analysis, functional groups of synthesized GBT were established. From the PL spectrum, oxygen vacancies in synthesized GBT were observed at 518 nm. Furthermore, the antibacterial and anticancer activities of GBT were evaluated.

***Key words*:** Ba, TiO_2, Green process, *Withania somnifera* hairy roots, Antibacterial, Anticancer activity

The manipulation of matter at the atomic, molecular, and nanoscale is known as nanotechnology. The properties offered by materials when viewed on a nanoscale are quite distinct from those provided by materials when viewed on a larger scale. Because of this, nanotechnology can enhance the qualities and properties of various things, including materials, electronic devices, biological systems, etc. [1]. The perovskite family has a high dielectric constant and a low loss, which makes it useful in capacitors, transducers, and multilayer capacitors [2]. The use of NPs as antimicrobial agents is a young and developing field, and the growing number of applications for NPs in nanomedicine - such as drug delivery systems, gene therapy, and diagnostic screening, lead the field. The particle size, stability, and concentration of metal oxide nanoparticles in the growth solution affect their ability to kill bacteria [3].

In addition, specific interactions between nanoparticles, which depend on the concentration of nanoparticles and the resistance of the microbes, can inhibit the growth rate of microbes when they grow in a medium amended with nanoparticles [4]. TiO_2 nanoparticles can be obtained through a wide variety of synthesis methods, including precipitation, hydrothermal, and solvothermal [5-6]. As part of these processes, several synthesis parameters are subjected to optimization and control to obtain TiO_2 NPs. Even though biological things can be used as an alternative to green chemistry to make safe and suitable nanoparticles for the environment [7-8], this article describes the synthesis of Ba-modified TiO_2 NPs from the extract of *Withania somnifera* hairy roots (WSR), as well as the studies that have been done to characterize the NPs. *Withania somnifera* (WS) is widely distributed in subtropical areas worldwide. WS is a versatile medicinal plant belonging to the *Solanaceae* family. Many illnesses, including fever, anticancer, diabetes, arthritis, heart issues, and piles, are treated with this plant [9]. Furthermore, the plant's withanolide alkaloids may be responsible for the plant's well-known anticancer, reduced the back pain relief, and muscle-strengthening properties. WS is also abundant in various highly valued secondary metabolites, including glycosides, alkaloids, flavonoids, phenolics, and steroids. Various parts of the plant have multiple preclinical trials, including cardioprotective, anticancer, antioxidant, antibacterial, antifungal, anti-inflammatory, hepatoprotective, anti-depressant, and low blood glucose effects [9]. The present work focuses on synthesizing Ba-modified TiO_2 NPs using an extract of WSR. This study aims to examine the structure, morphology, and antibacterial and anticancer activity of (GBT) green processed of Ba-modified TiO_2 nanoparticles in relation to human pathogens. The results were based on how much the bacteria's growth was stopped, how many exopolysaccharides they made, and their minimum inhibitory concentration (MIC).

Received: 05 Mar 2023; Revised accepted: 12 May 2023; Published online: 16 May 2023

Correspondence to: Appakan Shajahan, Plant Molecular Biology Laboratory, P. G. and Research Department of Botany, Jamal Mohamed College (Autonomous), Affiliated to Bharathidasan University, Tiruchirappalli - 620 020, Tamil Nadu, India, Tel: +91 94438 74731; E-mail: shajahan.jmc@gmail.com

Citation: Palusamy R, Ganesan T, Umaralikhan L, Shajahan A. 2023. Barium modified titanium dioxide nanoparticles prepared via a green process using *Withania somnifera* hairy roots. *Res. Jr. Agril. Sci.* 14(3): 711-715.

The outcomes of the tests show that the materials can inhibit these bacteria from growing, which makes them useful for commercial applications. Furthermore, the MTT assay was then used to conduct a preliminary in vitro assessment of cytocompatibility and cell viability.

MATERIALS AND METHODS

Barium nitrate (98%) and titanium isopropoxide were purchased from Sigma Aldrich.

Preparation of natural Withania somnifera *hairy roots (WSR) reduction agent*

The 5 g of dried *Withania somnifera* hairy roots (WSR) powder was mixed with 100 mL of deionized water. The *Withania somnifera* hairy roots (WSR) solution was boiled at 80 °C for 20 minutes on a magnetic stirrer. After that, the *Amomum subulatum Roxb* solution mixture was filtered using Whatman No. 1 paper. Filter WSR solution stored in the refrigerator.

Green synthesis of Ba modified TiO_2

To prepare Ba-modified TiO_2 (GBT) NPs, 0.010 M of barium nitrate solute was added to 0.090 M of titanium isopropoxide solution. Next, the Ti metal solution was added to 100 mL of WSR extract to produce a white, homogenous solution. This titanium precipitate solution was stirred continuously at 80 °C for 4-6 hours. The precipitate was then calcined at 700 °C for 5 hours.

Supporting information

Characterization techniques (SI 1), Antibacterial assay (SI 2), Cell culture maintenance (SI 3) MTT stock solution (SI 4), SI 5 MTT assay (SI 5), for GBT NPs are provided in Supporting Information (SI).

SI 1 characterization techniques

The GBT NPs were characterized by an X-ray diffractometer (model: X'PERT PRO PANalytical). The diffraction patterns were recorded in the 20°–80° for the GBT NPs, where the monochromatic wavelength of 1.54 was used. The samples were analyzed by field emission scanning electron microscopy (Carl Zeiss Ultra 55 FESEM) with EDAX (model: Inca).

The NanoPlus Dynamic Light Scattering (DLS) Nano Particle Sizer was used for the particle size analysis of the GBT NPs. The FTIR spectrum was recorded in the wavenumber range of 400–4000 cm-1 by using the Perkin-Elmer spectrometer. The UV-Vis-NIR spectrum was captured using Lambda 35 at wavelengths ranging from 200 to 1100 nm. Photoluminescence spectra were measured using the Cary Eclipse spectrometer.

SI 2 antibacterial assay

The antibacterial activity of the above GBT nanoparticles was investigated by the well diffusion method and tested against G+ (*S. aureus, S. pneumoniae and B. subtilis*) *G-bacteria (K. pneumoniae, E. coli* and *P. vulgaris*) after molten nutrient agar, according to the Clinical and Laboratory Standards Institute (CLSI). After inoculation, well loaded with 1, 1.5, and 2 mg/ml of the test samples were placed on the bacteria-seeded well plates using micropipettes. The plates were then incubated at 37 °C for 24 hours. The inhibition zone was measured. As a positive control for G+ and G-bacteria, amoxicillin (Hi-Media) was used.

SI 3 cell culture maintenance

Blood cancer cell (MOLT-4) lines were procured from the cell repository of the National Centre for Cell Sciences (NCCS), Pune, India. Dulbecco`s Modified Eagle Media (DMEM) was used for maintaining the cell line, which was supplemented with 10% fetal bovine serum (FBS). Penicillin (100 U/ml), and streptomycin (100 µg/ml) were added to the medium to prevent bacterial contamination. The medium with cell lines was maintained in a humidified environment with 5% CO_2 at 37°C.

SI 4 MTT stock solution

MTT (50 mg) dye was dissolved in 10 mL of PBS. After vertexing for 1 min, it was filtered through 0.45 micro filters. The bottle was wrapped with aluminium foil to prevent light, as MTT was light sensitive. The preparation was stored at 4 °C.

SI 5 MTT assay

Cell viability assay, Blood cancer cell (MOLT-4) cells were harvested and counted using haemocytometer diluted in DMEM medium to a density of 1×10^4 cells/ml was seeded in 96 well plates for each well and incubated for 24 h to allow attachment. After Blood cancer cell (MOLT-4) cells treated with control and the containing different concentrations of sample GBT NPs at 5 to 20 µg/ml were applied to each well. Blood cancer cell (MOLT-4) cells were incubated at 37°C in a humidified 95% air and 5% CO_2 incubator for 24 h. After incubation, the drug-containing cells wash with fresh culture medium and the MTT (5 mg/ml in PBS) dye was added to each well, followed by incubated for another 4 h at 37°C. The purple precipitated formazan formed was dissolved in 100 µl of concentrated DMSO and the cell viability was absorbance and measured 540 nm using a multi-well plate reader. The results were expressed at the percentage of stable cells with respect to the control. The half maximal inhibitory concentration (IC_{50}) values were calculated, and the optimum doses were analyzed at different time period.

$$\text{Cell viability (\%)} = \frac{\text{Mean absorbance of the control} - \text{Mean absorbance of the sample}}{\text{Mean absorbance of the control}} \times 100$$

The IC_{50} values were determined from the sample A and B dose responsive curve where inhibition of 50% cytotoxicity compared to vehicle control cells. All experiments were performed at least three times in triplicate.

RESULTS AND DISCUSSION

XRD patterns

XRD patterns of the synthesis of Ba doped TiO_2 NPs is shown in (Fig 1). X-ray diffraction peaks are located at angles (2θ) of 24.7, 27.5, 30.9, 38.2, 44.7, 55.6, and 65.3, which correspond to (001), (110), (111), (200), (211), and (220) PLANE of GBT nanoparticles, which exhibit rutile TiO_2 structure (JCPDs NO:75-1537). It is worth noting that no secondary peaks were observed. The average particle size of Ba-doped TiO_2 NPs is 35 nm.

Morphology and chemical composition

FESEM image of green synthesized GBT NPs is shown in (Fig 2). The GBT NPs formed grains in the spherical and bowl-like particles are randomly distributed and visible in SEM images. According to the FESEM image, the average particle size is about 50 nm. The results of the EDX analysis, which can be seen in (Fig 3), confirmed the presence of the elements Ba,

Ti, and O in the GBT NPs that had been synthesized. We could determine this sample's composition by looking at it in three different locations. They show reasonably identical values (within 0.01 at. %), demonstrating that the sample has a uniform composition as shown in (Fig 3). The elemental atomic composition reveals that Ba, Ti, and O each make up 24.23% of the total, 47.57% of the total, and 25.36% of the total, respectively. DLS is a method for studying the hydrodynamic particle size distribution of GBT nanoparticles. The average particle size was observed at 65 nm (Fig 4).

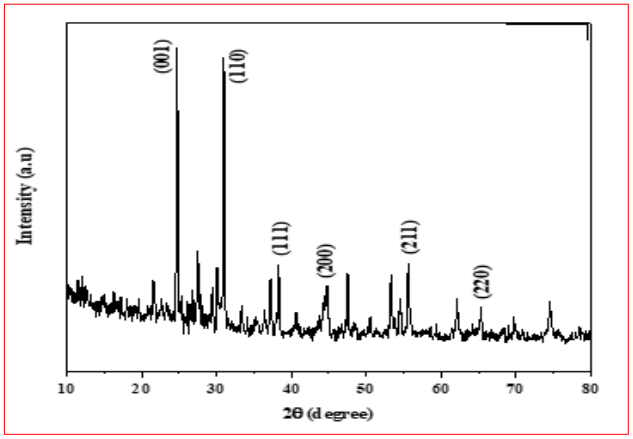

Fig 1 X-ray diffraction pattern of GBT NPs

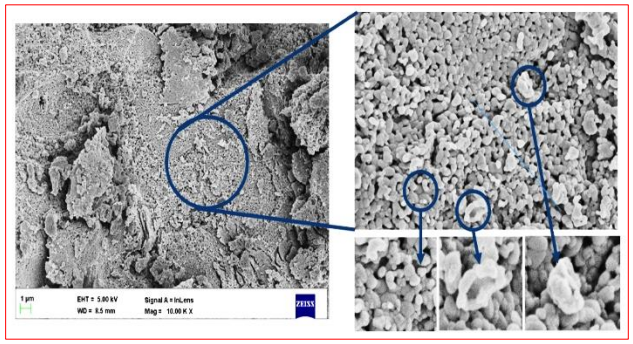

Fig 2 FESEM image of GBT NPs

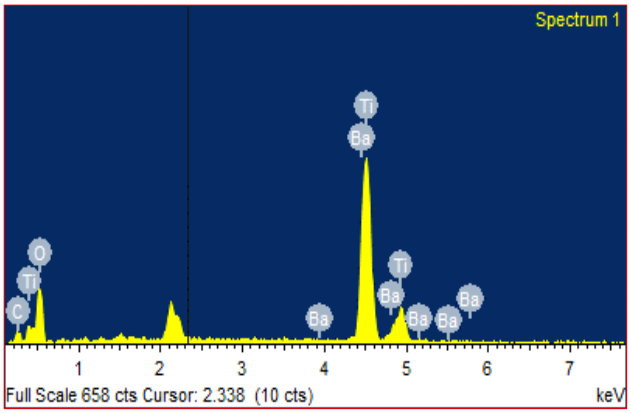

Fig 3 EDAX spectrum of GBT NPs

FTIR spectral and UV-Vis spectral analysis

At room temperature, FTIR spectra of the GBT sample were recorded for wavenumbers ranging from 4000 to 400 cm^{-1} (Fig 5). The vibrational peaks assigned to 446, 535, 848, 1421, 1642, 2922, and 3436 cm^{-1} are vibrational peaks of GBT showing stretching in Ti-O, Ti-OH, COO-, O-H, C-H and Ba-OH bonds.

The infrared absorption region corresponds to the region that spans from 400 to 600 cm^{-1}. Strong peaks can be seen at 446 cm^{-1} and 535 cm^{-1} due to Ti-O bending vibrations along the polar axis [11-13]. The bending vibrations in the COO- group caused by the plant's acid ligand are the source of the vibrational peaks measured at 848 and 1415 cm^{-1}, respectively. The H-O-H bending mode peaks at 1642 cm^{-1} and the O-H stretching mode is observed at 3436 cm^{-1} [14]. (Fig 6) depicts the UV-visible absorbance spectrum of green synthesis Ba-doped TiO_2 NPs. The GBT NPs exhibit a strong absorbance edge peak at 273 and 398 nm, which may be electron transfer from the valence band to the conduction band.

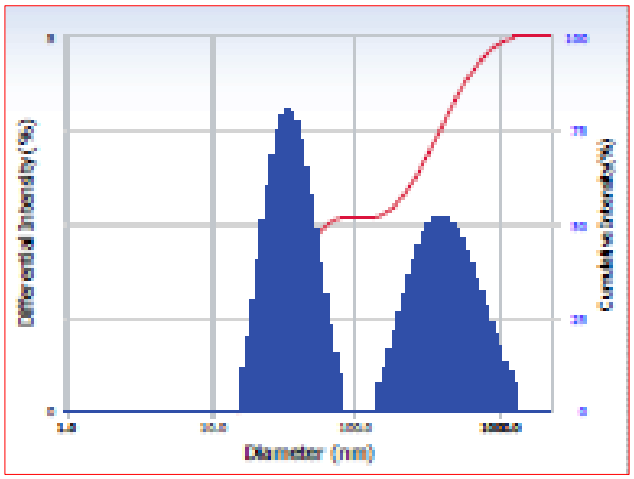

Fig 4 DLS spectrum of GBT NPs

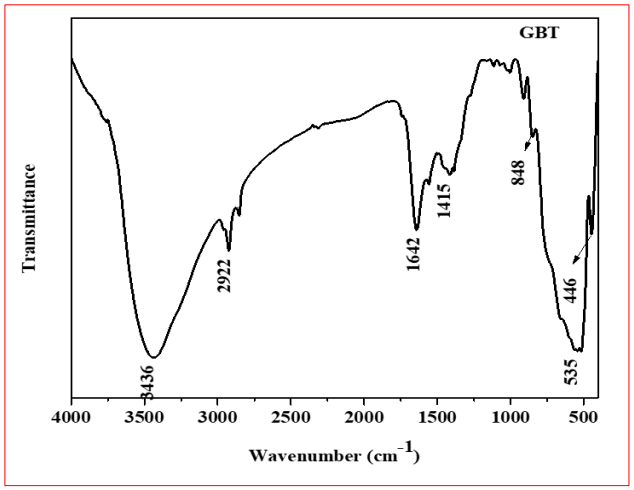

Fig 5 FTIR spectrum of GBT NPs

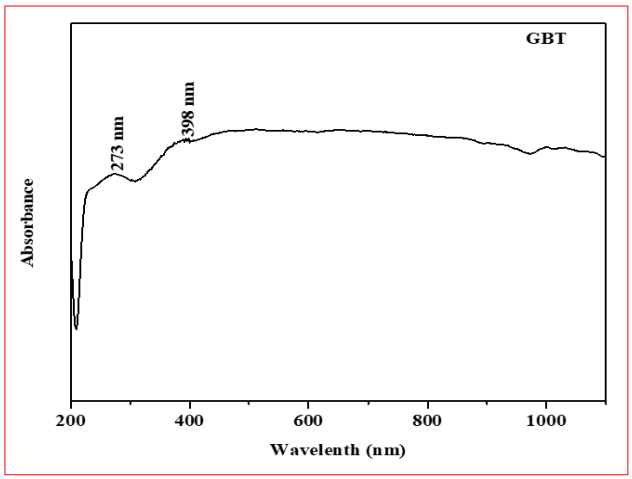

Fig 6 UV-Vis absorbance spectrum of GBT NPs

PL spectral analysis

The PL spectrum of the green synthesis of GBT NPs with an excitation wavelength of 325 nm is displayed in (Fig 7). Peaks in the GBT NPs spectrum were found at 375, 395, 405, 418, 451, 481, and 518 nm, respectively. UV emissions (near-

band edges) were discovered at 375 and 395 nm due to the free exciton-exciton collision process's radiative recombination. The violet emission observed at 405 and 418 nm is due to the electron transfer from the surface donor level of the tin interstitials (Ti_i) to the top level of the valence band. The blue emission bands observed at 451 and 481 nm are attributed to the singly ionized tin vacancies (V_{Ti}). The green emission band is centered at 517 nm due to oxygen vacancies (O_v) [8], [15-16].

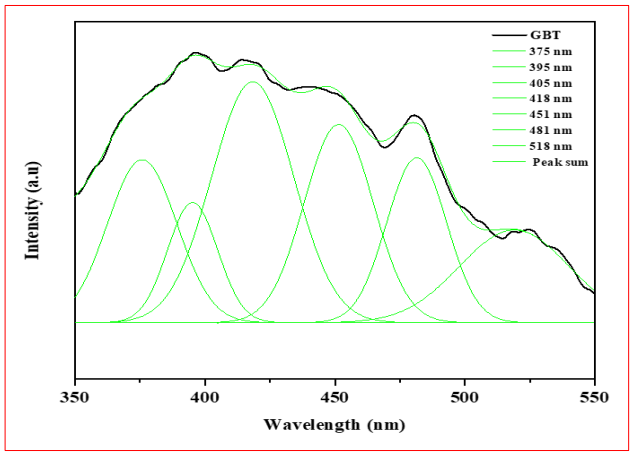

Fig 7 Photoluminescence spectrum of GBT NPs

Antibacterial activity

In terms of antibacterial activity, GBT NPs were tested against *S. aureus*, *S. pneumoniae*, *B. subtilis*, *K. pneumoniae*, *E. coli*, and *P. vulgaris* using the well diffusion method, as shown in (Fig 8). The Zone of Inhibition of GBT NPS and conventional antibiotics like amoxicillin show antibacterial activity as shown in (Fig 9). In order to increase the concentration of GBT NPs and also increase their antibacterial activity. Synthesized GBT NPs are very good against all bacterial pathogens; *B. subtilis* exhibits the highest inhibition rate compared to other gram-positive and gram-negative bacterial cultures.

In the current work, XRD measurements of the GBT particle size show that it is approximately 35 nm, and the surface defect (oxygen vacancies: O_v) of the GBT is demonstrated by the PL spectra at 518 nm. A nanomaterial often produces more ROS (Reactive Oxigen Species) if it has more vital photocatalytic activity and oxygen vacancies. In this example, water splitting inside the cell's cytoplasm may produce active free radicals such as singlet oxygen and hydroxide radicals. Single oxygen and hydroxide radicals, or ROS, interact with the DNA and lipid macromolecules found in bacterial cells, disrupting the physiological processes that are taking place inside the cell.

Anticancer activity

The anticancer activity assay of Ba-doped TiO_2 NPS was investigated on the viability of human blood cancer cell MOLT-4 cells at various concentrations, such as 2.5 to 15 µg/ml at 24 h at 37 °C. After incubation, cytotoxicity was tested using the MTT assay. (Fig 10) shows the MOLT-4 cell lines treated with GBT NPs demonstrated anticancer activity at all concentrations tested (2.5 to 15 g/ml). In addition, due to the cytotoxic inhibition activity of reactive oxygen species (ROS)-induced cell death, the IC50 estimates of cell inhibition of GBT NPs were observed to be 10.8 g/mL.

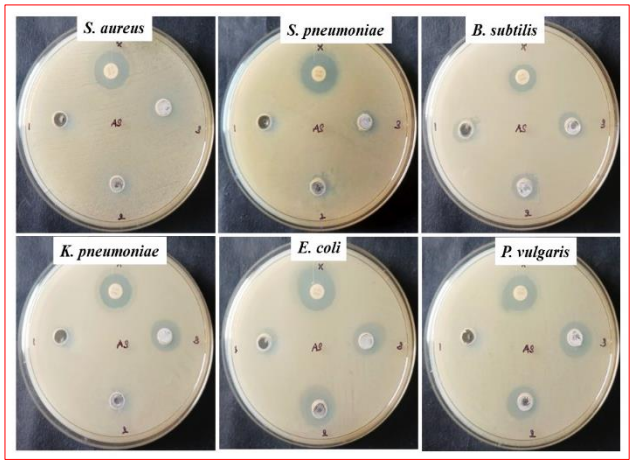

Fig 8 Antibacterial activity of GBT NPs treated with *S. aureus, S. pneumoniae, B. subtilis, K. Pneumoniae, E. coli* and *P. vulgaris* bacterial strain

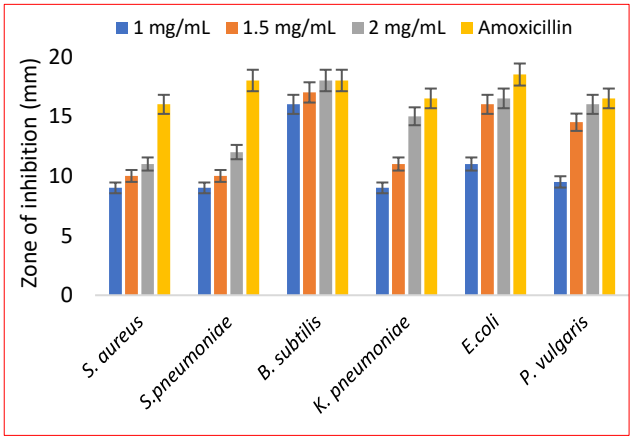

Fig 9 Zone of inhibiton of GBT NPs treated *with S. aureus, S. pneumoniae, B. subtilis, K. Pneumoniae, E. coli* and *P. vulgaris* bacterial strain

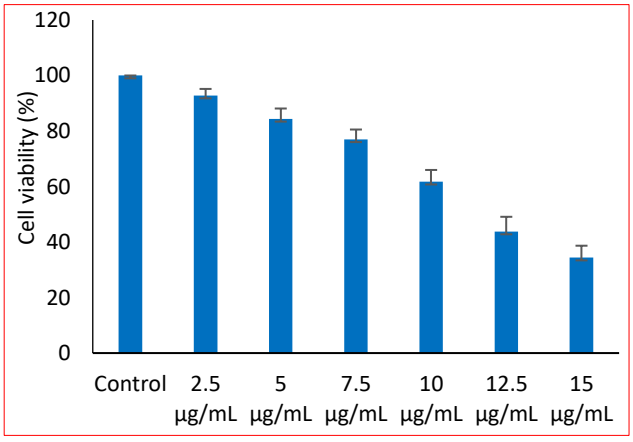

Fig 10 Anticancer activity of GBT NPs treated with blood cancer line (MOLT-4)

CONCLUSION

This study primarily focuses on the environmentally friendly plant-based synthesis of biomedically significant GBT using aqueous WRS, a significant plant in traditional medicine. The crystalline structure of the produced NPs has been confirmed by XRD analysis, and it is a tetragonal structure. SEM and EDX were used to determine the morphologies and elemental composition of synthesized GBT. EDX spectra confirm the presence and percentage of Ba (24.23%), Ti

(47.57%), and O (25.36%). DLS analysis reveals particle sizes as small as 65 nm. FTIR spectroscopy analysis verified the existence of phytochemicals in WRS present in the sample. The acid ligand of WRS (COO-) was obtained at 848 and 1415 cm^{-1}. It confirms the plant precursors are still available in synthesized GBT. The PL spectra showed that, primary electron transition takes place between inter-bands and direct bands, and it showed trap-state emission. The synthesized GBT NPs exhibit antibacterial potential against both G+ and G- bacterial strains. Increasing the concentration of GBT NPs also increased their anticancer activity against blood cancer cell lines.

Acknowledgement

Dr. Appakan Shajahan and authors thanks DST, Govt. of India for providing facilities through DST-FIST Program and DBT, Govt. of India for their support through star college scheme.

Ethics declarations: *None*

Competing interests

The authors declare no competing interests.

Availability of data and materials

All datasets generated or analyzed during this study are included in the manuscript.

LITERATURE CITED

1. Bayda S, Adeel M, Tuccinardi T, Cordani M, Rizzolio F. 2019. The history of nanoscience and nanotechnology: from chemical–physical applications to nanomedicine. *Molecules* 25(1): 112.
2. Zhang C, Li X, Ding L, Jin C, Tao H. 2022.Effect of BaTiO 3 powder as an additive in perovskite films on solar cells. RSC advances.;12(13):7950-60.
3. ud Din F, Aman W, Ullah I, Qureshi OS, Mustapha O, Shafique S, Zeb A. 2017. Effective use of nanocarriers as drug delivery systems for the treatment of selected tumors. *International Journal of Nanomedicine* 12: 7291.
4. Umaralikhan L, Jaffar MJ. 2016. Antibacterial and anticancer properties of NiO nanoparticles by co-precipitation method. *Journal of Advanced Applied Scientific Research* 1(4): 24-35.
5. Hayashi H, Noguchi T, Islam NM, Hakuta Y, Imai Y, Ueno N. 2010. Hydrothermal synthesis of BaTiO3 nanoparticles using a supercritical continuous flow reaction system. *Journal of Crystal Growth* 312(12/13): 1968-1972.
6. Beauger A, Mutin JC, Niepce JC. 1983. Synthesis reaction of metatitanate BaTiO 3: Part 1 Effect of the gaseous atmosphere upon the thermal evolution of the system BaCO 3-TiO 2. *Journal of Materials Science* 18: 3041-3046.
7. Umaralikhan L, Jamal Mohamed, Jaffar M. 2018. Green synthesis of MgO nanoparticles and its antibacterial activity. *Iranian Journal of Science and Technology, Transactions A: Science* 42: 477-485.
8. Umaralikhan L, Jaffar MJ. 2017. Green synthesis of ZnO and Mg doped ZnO nanoparticles, and its optical properties. *Journal of Materials Science: Materials in Electronics* 28: 7677-7685.
9. Saleem S, Muhammad G, Hussain MA, Altaf M, Bukhari SN. 2020. *Withania somnifera* L.: Insights into the phytochemical profile, therapeutic potential, clinical trials, and future prospective. *Iranian Journal of Basic Medical Sciences* 23(12): 1501.
10. Khan TM, Zakria M, Shakoor RI, Hussain S. 2016. Composite-hydroxide-mediated approach an effective synthesis route for BaTiO 3 functional nanomaterials. *Applied Physics A.* 122: 1-6.
11. Sipahioğlu S, Madakbaş S, Arda L, Esmer K. 2013. Structural and dielectric properties of two different BaTiO3/polyaniline nanocomposites. *Journal of Inorganic and Organometallic Polymers and Materials* 23(2): 333-339.
12. Bhuiyan MR, Alam MM, Momin MA, Uddin MJ, Islam M. 2012. Synthesis and characterization of barium titanate (BaTiO3) nanoparticle. *Int. Jr. Mater and Mech. Eng*. 1: 21-24.
13. Harizanov O, Harizanova A, Ivanova T. 2004. Formation and characterization of sol–gel barium titanate. *Materials Science and Engineering: B.* 106(2): 191-195.
14. Trivedi MK, Nayak G, Patil S, Tallapragada RM, Latiyal O, Jana S. 2015. Impact of biofield treatment on atomic and structural characteristics of barium titanate powder. *Industrial Engineering and Management* 4(3): 1000166.
15. Jiang S, Ren Z, Yin S, Gong S, Yu Y, Li X, Wei X, Xu G, Shen G, Han G. 2014. Growth and bending-sensitive photoluminescence of a flexible PbTiO3/ZnO nanocomposite. *ACS Applied Materials and Interfaces* 6(14): 10935-10940.
16. Choudhury B, Choudhury A. 2013. Oxygen vacancy and dopant concentration dependent magnetic properties of Mn doped TiO2 nanoparticle. *Current Applied Physics* 13(6): 1025-1031.